JACS
JOURNAL OF THE AMERICAN CHEMICAL SOCIETY

Article

pubs.acs.org/JACS

kinITC: A New Method for Obtaining Joint Thermodynamic and Kinetic Data by Isothermal Titration Calorimetry

Dominique Burnouf,[§] Eric Ennifar,[§] Sondes Guedich, Barbara Puffer,[‡] Guillaume Hoffmann, Guillaume Bec, François Disdier, Mireille Baltzinger,[†] and Philippe Dumas*

"Architecture et Réactivité de l'ARN", Biophysique et Biologie Structurale, Institut de Biologie Moléculaire et Cellulaire du CNRS, Université de Strasbourg, 15, rue René Descartes, 67084 Strasbourg, France

Supporting Information

ABSTRACT: Isothermal titration calorimetry (ITC) is the method of choice for obtaining thermodynamic data on a great variety of systems. Here we show that modern ITC apparatus and new processing methods allow researchers to obtain a complete kinetic description of systems more diverse than previously thought, ranging from simple ligand binding to complex RNA folding. We illustrate these new features with a simple case (HIV-1 reverse transcriptase/inhibitor interaction) and with the more complex case of the folding of a riboswitch triggered by the binding of its ligand. The originality of the new kinITC method lies in its ability to dissect, both thermodynamically and kinetically, the two components: primary ligand binding and subsequent RNA folding. We are not aware of another single method that can yield, in a simple way, such deep insight into a composite process. Our study also rationalizes common observations from daily ITC use.

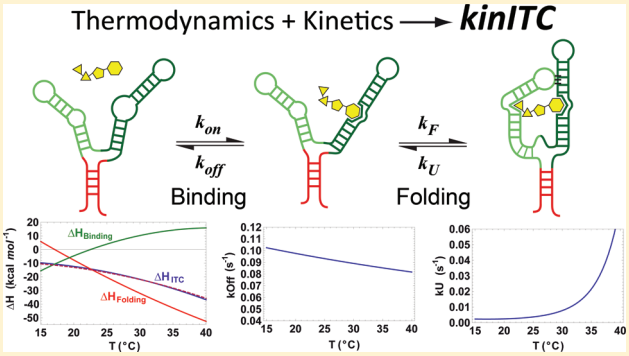

INTRODUCTION

Isothermal titration calorimetry (ITC), which measures directly the heat evolved during a reaction, is the method of choice for obtaining thermodynamic information. This is because only ITC allows researchers to obtain directly the variations of enthalpy ΔH and of entropy ΔS, as well as the dissociation constant K_d and the stoichiometry of binding, for an association/dissociation process. One major feature of modern instruments is their ability to measure heat powers as low as 0.1 μW (about the power received on a 1 m^2 receptor 10 km away from a 100-W light bulb!). Because of this high sensitivity, ITC has become an invaluable tool in biology to study association processes involving lipid membranes, proteins, nucleic acids, macromolecular assemblies of any kind, and a great variety of ligands.[1−3] Importantly, classical thermodynamics is concerned with transitions between well-defined states, but not at all with the kinetics of these transitions, and the results obtained classically by ITC do not give insight into this important aspect. However, as pioneered a long time ago by J. Sturtevant, it is possible to obtain kinetic information on enzymatic reactions (for a review, see ref 4). Typical examples of this method were obtained with NAD-NADase,[5] cytochrome *c* oxidase,[6] and hexokinase.[7] The methods in use were bound to conditions assuming that the reactions were of first-order. To our knowledge, no systematic attempt has been made to retrieve kinetic information on more diverse systems and in more general conditions. In this work, we expose new methods that we named "kinITC", for "kinetic ITC". They make use of the classical multiple injection method (MIM), wherein a compound present initially in the measurement cell (compound A) is mixed with a compound B injected in small amount at regular intervals. An example of such a titration is shown for an exothermic reaction in Figure 1 (left). Here, each negative "peak" corresponds to the heat power evolved in the measurement cell by the reaction between compounds A and B. Usually, these power peaks are integrated to obtain the heat

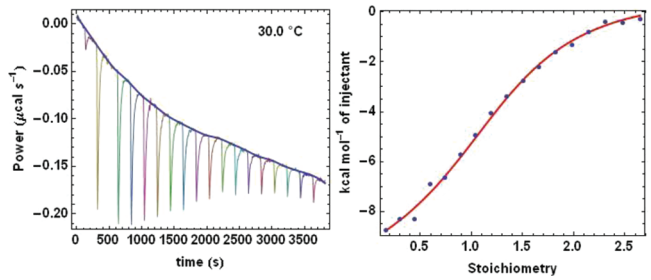

Figure 1. MIM results for Nevirapine binding to HIV-1 RT. (Left) Example of a raw titration curve with its baseline. See Figure S4 for all baseline-corrected curves, and Table 1 for all conditions. (Right) Integrated heats for each injection after baseline correction (dots) and theoretical curve obtained by the "global thermodynamic treatment".

Received: September 26, 2011
Published: November 29, 2011

   dx.doi.org/10.1021/ja209057d | J. Am. Chem.Soc. 2012, 134, 559−565

evolved at each titration step (Figure 1, right), which eventually yields the variation of enthalpy during the reaction along with the affinity and the stoichiometry of the interaction.[3] The aim of this work is to show how to process such titration curves to retrieve the kinetic information embedded in their shapes.

We start with a simplified analysis of the method for a situation described by the following simple scheme:

$$A + B \leftrightarrows C \qquad \text{with parameters } k_{on},\ k_{off} \tag{1}$$

for which $K_d = k_{off}/k_{on}$ is the dissociation constant. The simplification involved ignoring the time response of the instrument (τ_{ITC}) and the fact that compound B is not available instantaneously to react with compound A due to the finite injection and mixing times. This nevertheless gives results of practical interest. We then show how to obtain a realistic simulation of the successive injection curves by taking these two factors into account. These developments are applied in two different situations.

First, we considered a simple situation represented by eq 1 and corresponding to the interaction between HIV-1 reverse transcriptase (RT) and Nevirapine, which is the prototype of its non-nucleosidic inhibitors[8] (Figure S5A).

We next considered a more complicated situation illustrating well the originality of our new method. For that, we have studied the dynamics of interaction of the *Escherichia coli* riboswitch present in the 5′-UTR of the *thiC* mRNA with its thiamine pyrophosphate (TPP) ligand[9,10] (Figure S5B). This riboswitch uses a feedback mechanism to control the transcription of the downstream *thiC* gene involved in TPP synthesis.[11] The feedback mechanism results from the complete folding of the regulatory RNA triggered by TPP binding. It is anticipated that such a riboswitch is controlled kinetically, not thermodynamically, because the just-synthesized riboswitch has to arrest mRNA synthesis if it senses a sufficient level of TPP[12] (for a discussion of kinetic control, see ref 13).

Practically, the increased complication for the kinITC method arises from the need to consider two consecutive kinetic steps, ligand binding and RNA folding (Figure S5B):

$$R_0 + TPP \leftrightarrows R_1 \qquad \text{with parameters } k_{on},\ k_{off} \tag{2a}$$

$$R_1 \leftrightarrows R_1^* \qquad \text{with parameters } k_F,\ k_U \tag{2b}$$

where R_0 is the free unfolded RNA, R_1 is the still-unfolded RNA transiently bound to TPP, and R_1^* is the folded RNA more stably bound to TPP; k_F and k_U are for folding and unfolding, respectively. For the RT/Nevirapine as well as the TPP/riboswitch, we obtained a complete kinetic and thermodynamic description of the respective mechanisms. Our kinetic results were carefully assessed by independent means.

RESULTS AND DISCUSSION

Quantitative Results. All numerical results are provided in the Supporting Information, SI-15.

Results from a Simplified Analysis. Here we focus on the heat power $P_s(t)$ evolved in the measurement cell and not on $P_m(t)$, which is the power actually measured, as illustrated in Figure 1 (left). Therefore, the instrument response time τ_{ITC}, being only useful for estimating $P_m(t)$ from $P_s(t)$, is irrelevant at this stage. This first analysis (Materials and Methods) yielding $P_s(t)$ is simplified because it ignores the practical problems arising from the finite injection and mixing times of compound B (Supporting Information, SI-3). It nevertheless explains well the common observation of a variation in the equilibration time during successive injections (Figure S3A). It can be shown that this equilibration time θ starts from a minimum value θ_1 at the first injection and reaches its maximum at mid-titration ($\theta = \theta_{max}$), and that the ratio θ_{max}/θ_1 is well approximated by $c^{1/2}/2$, with c being the Wiseman parameter, $[A]_0/K_d$, with $[A]_0$ the initial concentration of compound A. Also of interest is the estimate $\theta_{max} \approx 2k_{off}{}^{-1}c^{-1/2}$. It is noticed that these two simple results can be used to quickly derive estimates of K_d, k_{on}, and k_{off} when there is a single binding site (Supporting Information, SI-4 and Figure S3A,B). A criterion was also obtained about the deleterious effect of the instrument response time, τ_{ITC} (Supporting Information, SI-5). This led us to define the dimensionless parameter Θ:

$$\Theta = (k_{on}k_{off}[A]_0)^{1/2}\tau_{ITC} = k_{off}\tau_{ITC}c^{1/2} \tag{3}$$

For the kinetic signal to emerge from the raw instrument response function, one should have $\Theta < \Theta_{max}$. The exact Θ_{max} value is not sharply defined. It essentially depends on the signal-to-noise ratio: with good-quality data, $\Theta_{max} = 2$ is likely to be a good rule of thumb, whereas noisier data will require a lower Θ_{max} value. It should be emphasized that this criterion ensures that the kinetic signal begins to emerge only when Θ is just less than Θ_{max}, which means that Θ values significantly lower than Θ_{max} should be considered in practice. This will be worth studying in more detail when a sufficient number of experimental examples are available. For the RT/Nevirapine interaction and the TPP riboswitch, the situation was quite favorable since Θ was less than 0.1 for the former and less than 0.2 for the latter at all temperatures.

kinITC Results with RT/Nevirapine Interaction. Because Nevirapine is hydrophobic, it was used as compound A to prevent any solubility problem. Three experiments were performed at 25, 30, and 35 °C (see Figure 1, Figure S4, and Table 1 for experimental conditions). Because of a rather low signal-to-noise ratio, the experimental curves were not of exceptional quality. This first example is thus representative of not-so-favorable situations. These curves were baseline-corrected (Supporting Information, SI-7 and Figure S4), and the global thermodynamic treatment (Materials and Methods) led to the results shown in Figure 2A. The kinetic treatment was then performed by considering arbitrarily k_{on} as unknown, and k_{off} was thus derived from $K_d = k_{off}/k_{on}$. The temperature variation of k_{on} was modeled with the Arrhenius equation. This led to a fit of the titration curves (Figure 3 and Supporting Information, SI-15 and Figure S6) with $k_{on}^0 \approx 1900\ M^{-1}\ s^{-1}$ (at $T^0 = 30$ °C) and $\Delta H_{on}^{\ddagger} \approx 16.5$ kcal mol^{-1} (1 cal = 4.184 J). The temperature variation of k_{on} and k_{off} and their Arrhenius plots are shown in Figure 2B. From this, we obtained $k_{off}^0 \approx 6 \times 10^{-3}$

Table 1. Experimental Conditions

	A (cell)	$[A]_0$ (μM)	B (syringe)	$[B]_0$ (μM)	δt^a (s)	δV^b (μL)
RT/ Nevirapine	Nevirapine	20	RT	243	5	2.33
RNA/TPP	RNA	30	TPP	300	1	1.5 or 1.2

[a]Time interval between successive measurements (integration time). [b]Injected volume at each injection (apart for the first one). All experiments were performed with the "high gain" mode and with the mixer rotating at 1000 rpm.

dx.doi.org/10.1021/ja209057d | J. Am. Chem.Soc. 2012, 134, 559−565

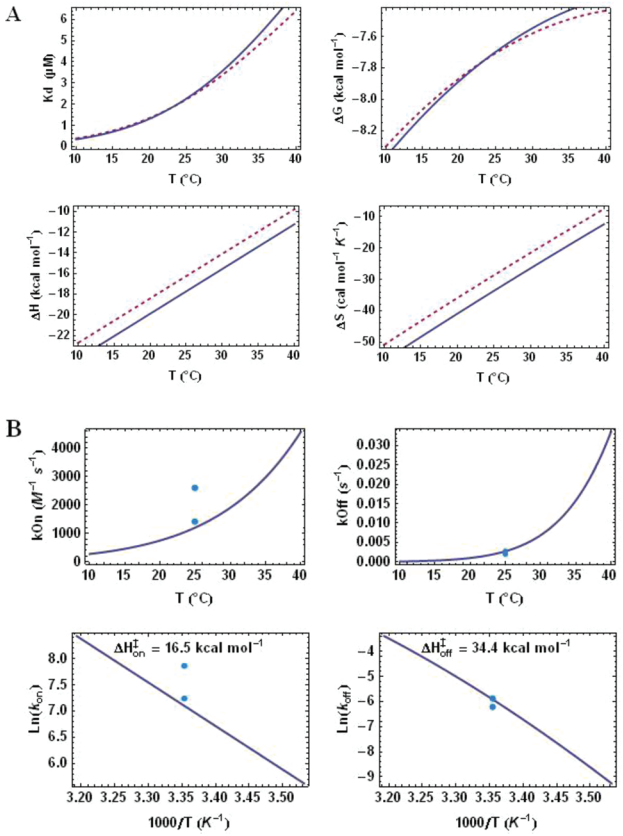

Figure 2. (A) Thermodynamic parameters for RT/Nevirapine interaction after the initial global treatment (dashed lines) and after fitting of all injection curves with the kinetic model (solid lines). The differences give an indication on the errors. (B) Kinetic parameters k_{on} and k_{off} and their Arrhenius plots after fitting of all injection curves (Figure 3, Figure S6). The blue dots correspond to independent results from SPR at 25 °C.

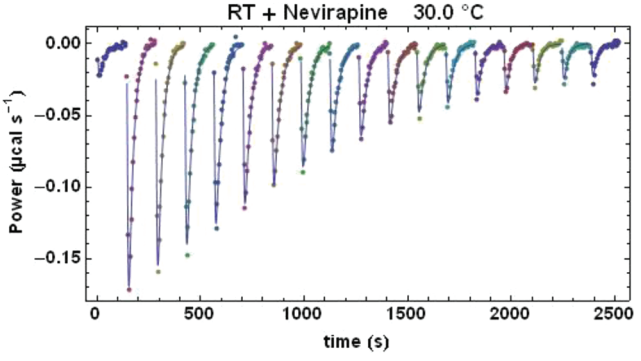

Figure 3. Fit of one experimental curve with the kinetic model. Other curves are shown in Figure S6. Note that only the part used in the fitting procedure for each injection is shown.

s^{-1} and $\Delta H^{\ddagger}_{off} \approx 34.4$ kcal mol^{-1}. Interestingly, we obtained almost identical results by repeating the calculations with only the two data sets at 25 and 35 °C (Supporting Information, SI-15), which illustrates that in this case the kinetic parameters are over-determined with three different temperatures.

A subtlety has to be stressed here. Indeed, the difference between the two activation enthalpies $\Delta H^{\ddagger}_{on}$ and $\Delta H^{\ddagger}_{off}$ has to be equal to ΔH; therefore, a constant value for each term (respectively, 16.5 and 34.4 kcal mol^{-1}) cannot rigorously account for a ΔH that is variable with the temperature (ΔC_p = 430 cal mol^{-1} K^{-1}). On one hand, the method in use does ensure that $\Delta H^{\ddagger}_{on} - \Delta H^{\ddagger}_{off} = \Delta H$ holds rigorously at all temperatures. This is apparent in our results with the curved Arrhenius plot for k_{off} (Figure 2B). On the other hand, a limit of the method is reached here since, had we decided to consider arbitrarily k_{off} as unknown instead of k_{on}, we would have met an opposite situation leading to a linear Arrhenius plot for k_{off} and a curved one for k_{on}. Therefore, in the absence of additional information, we only know how the difference $\Delta H^{\ddagger}_{on} - \Delta H^{\ddagger}_{off}$ varies with the temperature, but we cannot say anything about each term separately. As done usually, we can thus only report temperature-independent values for $\Delta H^{\ddagger}_{on}$ and $\Delta H^{\ddagger}_{off}$.

To assess these results, we used surface plasmon resonance (SPR). Two independent experiments were performed at 25 °C (Figure S10). The two k_{off} values from SPR are in excellent agreement with kinITC (Figure 2B and Supporting Information, SI-15), and the two k_{on} values (2600 and 1400 M^{-1} s^{-1}) also confirmed well the order of magnitude obtained by kinITC (1200 M^{-1} s^{-1}). Considering first the range of possible values for such a kinetic parameter (diffusion-controlled k_{on} values can be as high as 10^9 M^{-1} s^{-1}) and second that this RT/Nevirapine system was not very favorable for SPR (low MW of the ligand and possible heterogeneity that can occur due to covalent amine coupling of the protein on the chip), the difference observed between these two independent SPR k_{on} values is not crucial. Our SPR results are also consistent with those obtained in an analogous study.[14]

Interestingly, the low k_{on} value and the significant activation enthalpy values (particularly 34.4 kcal mol^{-1} for $\Delta H^{\ddagger}_{off}$) are consistent with the fact that the Nevirapine binding site does not pre-exist within the apo-RT,[15] which means that movements are necessary to create an input/output channel and the binding site itself (Figure S5A).

kinITC Results with the TPP Riboswitch. The RNA was used as compound A. Titrations were performed at 20, 27, 30, 34, and 37 °C (see Table 1 for experimental conditions). The quality of the data was excellent due to the good signal-to-noise ratio (Figure 4, Figure S8). A global thermodynamic treatment

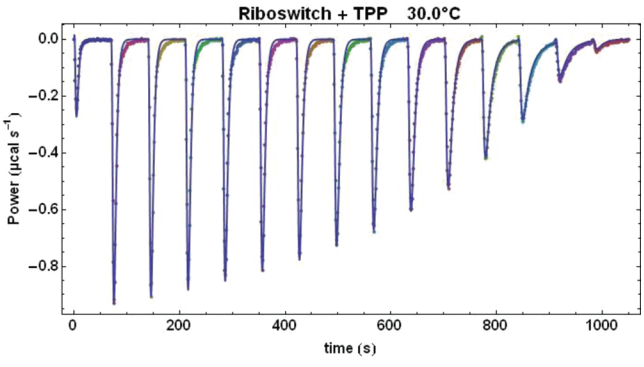

Figure 4. Fit of one baseline-corrected experimental curve with the kinetic model. The other curves are shown in Figure S8.

was first performed (Figure 5A). The resulting values for ΔH_{ITC} and K_{ITC} are in reasonable agreement with those obtained at 30 °C for the closely related *thiM* TPP riboswitch.[16] Our more complete data revealed unambiguously that $\partial \Delta C_p / \partial T = \alpha \neq 0$ ($\alpha \approx -60$ cal mol^{-1} K^{-2}). As for protein folding/unfolding, it is usually considered that $\Delta C_p \neq 0$ is linked (at least in part) to a variation in the hydration pattern,[17] albeit in a nonobvious way for nucleic acids.[18] In the present case, the fact

dx.doi.org/10.1021/ja209057d | J. Am. Chem.Soc. 2012, 134, 559–565

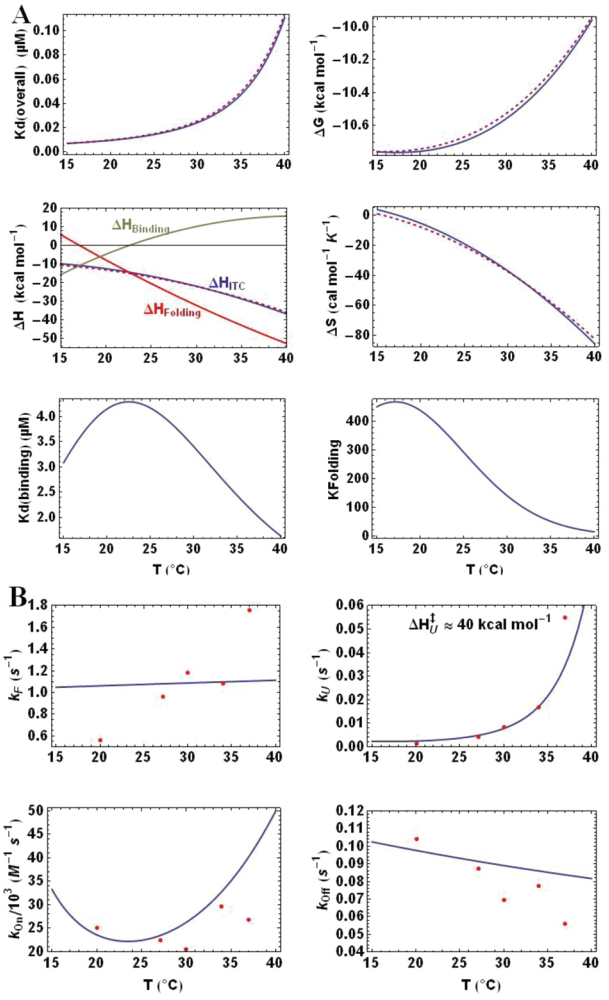

Figure 5. (A) Thermodynamic parameters for the TPP riboswitch after the initial global treatment (dashed lines) and after fitting of all injection curves with the kinetic model (solid lines). The figure for ΔH also shows the contributions from primary TPP binding and RNA folding to ΔH measured by ITC ($\alpha = \partial\Delta C_p/\partial T \approx -55$ cal mol^{-1} K^{-2}). (B) Kinetic parameters of eqs 2a and 2b) after fitting all injection curves (Figure 4, Figure S8) with k_{off} and k_F modeled with the Arrhenius equation. The value $\Delta H_U \approx 40$ kcal mol^{-1} was estimated from the resulting variation of $k_U(T)$. The red dots correspond to the results obtained by considering individual values for k_{off} and k_F at each temperature. The differences between these results are a mark of the correlations between parameters to be determined and of the accuracy. The independent kinetic values from SPR cannot be represented on these graphs since they correspond to global terms (eqs 4a and 4b).

that ΔC_p itself is markedly temperature-dependent is unusual and deserves additional investigations. Also, there is a temperature of maximum stability (ΔG minimum, $\Delta S = 0$) of the folded state around 15 °C. This possibility, linked to C_p(folded) < C_p(unfolded), is well known for proteins, but much less for RNA.[18] Therefore, such a global thermodynamic treatment of titration curves at several temperatures yield a wealth of information.

The kinetic treatment was performed by considering as unknown $\Delta H_{folding}$, and k_{off} and k_F of eqs 2a and 2b. The two kinetic parameters were modeled either by using the Arrhenius equation or by using individual values at each temperature. The procedure started with a manual search for a first set of values and continued by least-squares fit of all experimental curves (Figure 4, Figure S8).

This led to the results shown in Figure 5. It is not obvious at all to obtain in a different way the partition of the global enthalpic term ΔH_{ITC} into $\Delta H_{binding}$ and $\Delta H_{folding}$. Therefore, we cannot present an independent confirmation of this partition. According to it, there is an unfavorable binding component ($\Delta H_{binding} > 0$ above 22 °C). This positive value is consistent with the 3D structures of the closely related TPP riboswitches from *A. thaliana thiC*[19] and *E. coli thiM*.[11] Both structures show that TPP binding requires the opening of two adjacent bases to allow the stacking of the aromatic ring of the thiamine moiety. The overall favorable enthalpic term would thus result from its RNA-folding component. It is also difficult to obtain independent estimates of $K_{binding}$ and $K_{folding}$. We note that the global K_d obtained by ITC (i.e. $K_{d(ITC)} = 1/K_{ITC} \approx 25$ nM at 30 °C) is well below the TPP concentration in the cells that ranges roughly from 3 to 140 μM, depending on the growing media in use.[20−22] This is definitely in favor of a kinetic regulation of the switch since, at equilibrium, the riboswitch would always be saturated by TPP. Interestingly, our result shows that the K_d corresponding to the primary binding (i.e., $1/K_{binding}$, eq 2a) lies exactly in the lower limit range of 3 μM (Figure 5A), which indicates that this primary binding step is well tuned for sensing a variation of TPP concentration around its minimum value in the cell (see the Conclusions).

To obtain an independent experimental determination of the folding rate k_F, we used the classical technique of hydroxyl radical footprinting with a quench-flow.[23] In short, highly reactive OH$^\bullet$ radicals can be produced at will by the Fenton reaction during a very short time (15 ms). These radicals cleave the DNA or RNA backbone according to the accessibility of the hydrogen atoms of each (deoxy)ribose.[24] Hence, the variation of the RNA cleavage pattern obtained at various times after addition of TPP reflects the kinetics of RNA folding (Figure S9). We processed these experimental data with the kinetic model described in eqs 2a and 2b (to be published), which yielded $k_F = 1.1 \pm 0.3$ s^{-1} at 27 °C, in good agreement with the kinITC value (Figure 5B).

In contrast to k_F, which is well determined by such footprint experiments, k_{on} is poorly determined because only a few residues are involved in the primary step of TPP binding. We thus relied again upon SPR. However, with no SPR signal associated with RNA folding, SPR can only yield information on "global binding", exactly as does ITC when the information embedded in the shapes of the titration curves is ignored. The corresponding kinetic parameters k_{on}(global) and k_{off}(global) are related to those of eqs 2a and 2b by

$$k_{on}(\text{global}) = k_{on}k_F/(k_{off} + k_F) \quad (4a)$$

$$k_{off}(\text{global}) = k_{off}k_U/(k_{off} + k_F) \quad (4b)$$

These estimates result from the usual assumption that the intermediate species R_1 in eqs 2a and 2b is in quasi-equilibrium with R_0 and R_1*.

The result for k_{off}(global) from four independent SPR experiments at 25 °C (Figure S11) was $(2.94 \pm 0.3) \times 10^{-4}$ s^{-1}, in perfect agreement with that expected from kinITC (2.9×10^{-4} s^{-1}), but the result for k_{on}(global) was $(1.26 \pm 0.11) \times 10^5$ M^{-1} s^{-1}, which is in 6-fold excess vs the expected value from kinITC (2×10^4 M^{-1} s^{-1}). There is no way of explaining the kinITC results with such a value. We note however two facts: first, that SPR confirmed the k_{off}(global) obtained by kinITC

dx.doi.org/10.1021/ja209057d | J. Am. Chem.Soc. 2012, 134, 559−565

and, second, that K_d(ITC) = k_{off}(global)/k_{on}(global) cannot be in error by a factor of 6 due to the good quality and the high redundancy of the data. Therefore, if the K_d and k_{off}(global) values obtained by kinITC are correct, then k_{on}(global) from kinITC is also correct. Alternatively, if the latter conclusion is not exact, then one has no other choice than to conclude that both SPR and kinITC were wrong in reporting an identical k_{off}(global) value. We thus think that, most likely, all kinetic parameters were correctly obtained by kinITC. Another argument in favor of this conclusion is that different results were obtained by classical solution studies and SPR studies.[25−27] Importantly, these SPR studies often reported a lower K_d value than that obtained by ITC, exactly as observed in our case.

CONCLUSIONS

We have shown that kinITC could provide us with thermodynamic and complete kinetic data for the two studied systems. For the more complex riboswitch case, the assessment of these results by independent means support reasonably well the other "unusual" results on $K_{binding}$, $K_{folding}$ that are difficult to obtain independently, and on $\Delta H_{binding}$, $\Delta H_{folding}$ for which we are not aware of an alternative method for their determination. In the absence of independent information on these results, we can only examine whether they are meaningful. As mentioned earlier, that the term $\Delta H_{binding}$ was shown to become positive above 22 °C is in good agreement with the base unstacking necessary for the first step of TPP binding. Our kinetic results also highlight a dual functioning of the switch. It was already clear that this TPP riboswitch is under kinetic control, based on the fact that the global K_d is much lower than the usual TPP concentration in the cells. This is now more firmly established by the fact that the k_{off}(global) value that we obtained (3×10^{-4} s^{-1} at 25 °C) corresponds to a characteristic time of TPP release of ca. 1 h, which is much longer than the time necessary for the RNA polymerase to complete the riboswitch synthesis. According to ref 13, this is the hallmark of kinetic control of the ability to arrest mRNA transcription.[28] However, our results also show that, based on the much higher K_d value for the primary TPP binding, the riboswitch is thermodynamically driven for its ability to detect a low cellular TPP concentration. Therefore, in pictorial terms, this TPP riboswitch seems to function as a mouse-trap, but as one that would trap its prey only when the "mice are in sufficient number".

We think kinITC is a promising tool of general interest for obtaining information unattainable by other simple means. One should not exclude that the treatment performed for the TPP riboswitch, for which two obvious kinetic steps exist, might be extended to other cases. For example, we described the RT/Nevirapine interaction with a single kinetic step, but the low k_{on} value that was obtained results from a necessary conformational change of the RT to create the input channel and the binding site itself. This would correspond to an additional kinetic step, and kinITC could possibly resolve it. However, the low signal-to-noise ratio in this case might limit our ability to obtain more information (which we have not yet examined). Furthermore, in the present state of development of the new method, such results would need to be assessed by independent means. Also, a problem is particularly apparent in that the riboswitch results showed a slight but systematic disagreement between experimental and theoretical curves (Figure 4, Figure S8). If this is not due to inaccuracy in baseline correction (which seems unlikely in this case) or in the kinetic model, then this points to the need for a more sophisticated analysis of the instrument response time. In the latter situation, this would likely require knowledge of the hardware itself. Finally, we have presented here the use of kinITC with MIM, but it may be that the single injection mode is sufficient in favorable circumstances, which we are currently examining.

MATERIALS AND METHODS

Simplified Presentation of the kinITC Method. To avoid nonessential complications, we first expose a simplified version of the methodology for a single kinetic step reaction: A + B ⇄ C (we will later examine a more complicated situation with two consecutive kinetic steps). During a MIM classical ITC experiment, compound A present in the measurement cell (at an initial concentration $[A]_0$) is mixed with compound B (at a concentration $[B]_0$) injected in small amounts at regular intervals. The shape of each power curve following an injection is governed by the kinetics of equilibration, that is, by the differential equation,

$$dC/dt = k_{on}[A]_0 AB - k_{off}C \quad (5)$$

where k_{on} and k_{off} are the forward and backward kinetic rates (which allows defining $K_d = k_{off}/k_{on}$), and A, B, and C are the reduced concentrations, $[A]/[A]_0$, $[B]/[A]_0$, and $[C]/[A]_0$. Using reduced concentrations makes it possible to avoid doing numerical calculations with small numbers, which may be a cause of loss of precision. Together with conservation equations, equation (5) leads for the first injection ($C(0) = 0$) to

$$C(t) = B_0(1 - e^{t/\tau})/(C_2 - C_1 e^{t/\tau}) \quad (6)$$

with $B_0 = [B]_0/[A]_0$, $\tau^{-1} = k_{on}[A]_0(C_1 - C_2)$, and C_1, C_2 being the roots of the equation $[A]_0(1 - C)(B_0 - C) - K_dC = 0$ (with $C_1 > C_2$). Analogous solutions are readily obtained for the following injections (Supporting Information, SI-4). This simple analysis allows us to obtain the heat power evolved in the measurement cell:

$$P_s(t) = V_{cell}\Delta H[A]_0\, dC/dt \quad (7)$$

Realistic Simulation of a Titration Curve. The previous result on $P_s(t)$ does not correspond to the actually measured power $P_m(t)$ for two reasons. First, the evaluation of $P_s(t)$ is only ideal because the finite injection time and finite mixing times of compound B were not taken into consideration. Second, one also has to take into account the time response τ_{ITC} of the instrument to obtain $P_m(t)$ from $P_s(t)$. These factors, however, can be accounted for by using standard methods in signal processing, which allows us to obtain a good estimate of $P_m(t)$ from $P_s(t)$ (Supporting Information, SI-2). With the new-generation instrument that we used (ITC_{200} from Microcal, GE-Healthcare, Northampton, MA), the cell volume is small (203 μL) and $\tau_{ITC} \approx 3.5$ s (Figure S1), which is considerably less than the response time reported for older-generation instruments (15 s).[2]

Global Thermodynamic Treatment of Data at Several Temperatures. To obtain thermodynamic *and* kinetic information in general situations, one has to rely on a convincing fit of experimental titration curves. To overcome the serious problem of correlation between parameters, we perform experiments at different temperatures, enforcing a single set of parameters to allow fitting *all* injection curves of *all* experiments. However, one has first to obtain excellent knowledge of all thermodynamic data that are essential for tightly constraining the kinetic parameters (we recall that $K_d = k_{off}/k_{on}$ should hold at any temperature and that the evolution of $K_d(T)$ is governed by ΔH). We therefore process the data by considering the integrated heats for each injection (as done usually), but we do not process each temperature separately. Instead, we perform a "global thermodynamic treatment", which means that a single set of parameters has to allow fitting at once all titration curves, such as those of Figure 1 or Figure S7. To reduce the number of free parameters, we use the Van't Hoff equation to obtain an explicit function $K_d(T)$ (Supporting Information, SI-6). With this method, K_d is no longer a free parameter, except for a single value, K_d^0, at a

dx.doi.org/10.1021/ja209057d | J. Am. Chem.Soc. 2012, 134, 559−565

reference temperature T^0. Most often, $\Delta C_p = \partial \Delta H/\partial T$ is constant to a good approximation, which means that just three free parameters ($\Delta C_p = \Delta C_p^0$, ΔH^0, and K_d^0) should be sufficient to yield a complete description of the variation with temperature of all thermodynamic quantities: ΔH, K_d, $\Delta G = RT \ln K_d$, and $\Delta S = -\partial \Delta G/\partial T$. In particular situations like that of the TPP riboswitch, one has to consider an additional term, $\alpha = \partial \Delta C_p/\partial T$, to account for a significant variation of ΔC_p with the temperature. Very often, it is also needed to take into account an "active fraction" of the macromolecules for their ligand-binding ability. An example of a joint fit of several titration curves is shown for the TPP riboswitch (Figure S7), and the results are shown for RT/Nevirapine (Figure 2A) and TPP riboswitch (Figure 5A). Independent of any kinetic considerations, this global thermodynamic treatment is a new way of processing simultaneously titration curves obtained at different temperatures.

Linking Thermodynamic and Kinetic Parameters. The kinetic parameters k_{on} and k_{off} are linked to thermodynamics by $K_d(T) = k_{off}(T)/k_{on}(T)$, which means that either k_{on} or k_{off} only remains to be determined since $K_d(T)$ is known from the Van't Hoff equation. In situations where the Arrhenius equation describes well the temperature variation of this still undetermined parameter (for example, k_{on}), one has

$$k_{on}(T) = k_{on}^0 \exp[-(\Delta H_{on}^{\ddagger}/R)(1/T - 1/T^0)] \quad (8)$$

Therefore, five parameters (ΔC_p^0, ΔH^0, K_d^0, $k_{on}^0 = k_{on}(T^0)$, and the activation enthalpy $\Delta H_{on}^{\ddagger}$) have to be determined to fit altogether as many titration curves as desired. It should be emphasized that ΔC_p^0, ΔH^0, and K_d^0 are completely determined by the integrated power curves (which ignores their shapes), whereas k_{on}^0 and $\Delta H_{on}^{\ddagger}$ alone have to account for the shapes of all these power curves, which is a severe test of consistency. In other words, the fitting of the shapes of many injection curves is strongly over-determined. This fact is very important, as it is at the basis of the success of the method. A good illustration of it is given by the RT/Nevirapine case that yielded almost identical results by considering only the two extreme temperatures, 25 and 35 °C, instead of 25, 30, and 35 °C. Obviously, in situations like that of the TPP riboswitch with a nonconstant value of ΔC_p, more than two temperatures are needed to define correctly the curvature of the function $\Delta H(T)$. Furthermore, the TPP riboswitch also required more experimental data than RT/Nevirapine because the kinetic model was also more complicate. This model is detailed in the following.

Extension to Two Kinetic Steps. This situation is illustrated in this work with RNA folding triggered by the binding of a ligand (eqs 2a and 2b; Figure S5B). In such a case, one has to consider two coupled differential equations to describe the evolution of concentrations:

$$dR_0/dt = -k_{on}[R]_{tot}R_0L + k_{off}R_1 \quad (9a)$$

$$dR_1^*/dt = k_F R_1 - k_U R_1^* \quad (9b)$$

where $[R]_{tot}$ is the total RNA concentration, and R_0, L, and R_1^* are, respectively, the time-dependent reduced concentrations $[R_0]/[R]_{tot}$, $[L]/[R]_{tot}$, and $[R_1^*]/[R]_{tot}$. These differential equations have to be supplemented with conservation equations:

$$R_0 + R_1 + R_1^* = 1 \quad (10a)$$

$$R_1 + R_1^* + L = L_0 = [L]_{tot}/[R]_{tot} \quad (10b)$$

where $[L]_{tot}$ is the total TPP concentration. In addition, each step has its own equilibrium constant, $K_{binding} = k_{on}/k_{off}$ (in M^{-1}) and $K_{folding} = k_F/k_U$, and the two are linked to the global equilibrium constant attainable by ITC: $K_{ITC} = K_{binding}K_{folding}$ (in M^{-1}). Analogously, each step also has its own enthalpic contribution, respectively $\Delta H_{binding}$ and $\Delta H_{folding}$, and their sum has to correspond to the global enthalpic term measured by ITC: $\Delta H_{ITC} = \Delta H_{binding} + \Delta H_{folding}$ (which implies $\Delta C_{p,ITC} = \Delta C_{p,binding} + \Delta C_{p,folding}$). The Van't Hoff equation applies separately for each step, which means that the temperature variations of $K_{binding}$ and $K_{folding}$ are linked, respectively, to $\Delta H_{binding}$ and $\Delta H_{folding}$. Note that this automatically implies that K_{ITC} also varies with the temperature, in agreement with ΔH_{ITC}. Therefore, the Van't Hoff equation links tightly the different affinity constants (and thus their related kinetic parameters) to the measured enthalpy, which is of utmost importance for the success of the method. Finally, eq 6 should be replaced with

$$P(t) = V_{cell}(-\Delta H_{binding}\, d[R_0]/dt + \Delta H_{folding} d[R_1^*]/dt) \quad (11)$$

The minus sign before $\Delta H_{binding}$ results from the opposite variations of $[R_0]$ and $[R_1^*]$ when each step is going forward.

Computational Aspects. All method developments and programming were done with Mathematica V8 (Wolfram Research, Champaign, IL). A Web site (http://www-ibmc.u-strasbg.fr:8080/webMathematica/kinITCdemo/) illustrating several aspects of kinITC was setup with WebMathematica. More details about the fitting of titration curves are given in the Supporting Information, SI-8.

Summary of Experimental Conditions for kinITC. Buffer for RT/Nevirapine: Mes-NaOH 10 mM, pH 6.5, NaCl 100 mM, $MgCl_2$ 2 mM. Buffer for the TPP riboswitch: sodium cacodylate 50 mM, pH 6.5, potassium acetate 100 mM, magnesium acetate 5 mM.

Preparation of RT. The RT for kinITC and SPR experiments was prepared as described.[29]

SPR Experiments. SPR experiments were performed on a BIAcore2000 instrument (GE Healthcare). The kinetic analysis of HIV-1 RT/Nevirapine interaction was performed with sensor surfaces prepared using CM5 sensor chips (research grade) and amine coupling chemistry as described.[14,30] Kinetic experiments were performed at 25 °C using 10 mM Hepes, 150 mM NaCl, 3.4 mM EDTA, 0.01% surfactant P20 (polysorbate Tween20), DTT 1 mM, 4% DMSO, pH 7.5 as running buffer. The inhibitor Nevirapine was serially diluted in running buffer to working concentrations and injected for 1 min at a flow rate of 50 μL min^{-1} over the reference and RT surfaces. The dissociation phase was set to 10 min. Data were double-referenced and corrected for DMSO solvent effect. The data were fit with the software BIAevaluation (Figure S10), which yielded $k_{on} = 2.4 \times 10^3$ M^{-1} s^{-1} and $k_{off} = 1.5 \times 10^{-3}$ s^{-1}.

The TPP/riboswitch interaction was studied using CM5 sensor chips coated with streptavidin by amine coupling using the BIAcore amine coupling kit according to manufacturer's instructions. Approximately 7000−8000 RUs of streptavidin were attached on the CM5 chip.

To allow the binding of the RNA aptamer domain on the chips, a T7 promoter and a polyT sequence (5′ GGGTAATACGACTCACTATAGGGTTTTTTTTTTTTCAAC-aptamer 3′, from IDT) were introduced by PCR upstream of the aptamer. The PCR products were purified on a monoQ column (Pharmacia) with a NaCl gradient and further transcribed *in vitro* by T7 RNA polymerase according to the usual procedures. The RNA products were purified on a PA100 column (Dionex), eluted with $NaClO_4$, and the purified fractions were desalted and concentrated on Centricon 10K (Millipore). Purified RNA (10 μM) was heat-denaturated for 1 min at 90 °C and further renatured in buffer containing 50 mM sodium cacodylate pH6.5, potassium acetate 100 mM, and magnesium acetate 5 mM for 45 min at 25 °C. The renatured aptamer was then hybridized for 30 min at 37 °C to a 3′-biotinylated oligonucleotide (5′ AAAAAAAAAAAA-iSp9-biotin 3′, from IDT) at a ratio RNA/oligo = 1.5. This material was loaded on the SPR chip, and 1500−1800 RUs of biotinylated RNA were then immobilized on the streptavidin surface.

Kinetic titrations experiments were performed at 25 °C using 50 mM sodium cacodylate, pH 6.5, 100 mM potassium acetate, and 5 mM magnesium acetate as running buffer. The TPP was serially diluted in running buffer to working concentrations. Within a single binding cycle, the samples were injected sequentially in order of increasing concentration over both the reference and RNA surface. Prior to and after the binding cycle, buffer was injected to obtain "blank" responses essential for double-referencing the data. TPP was injected at 50 μL min^{-1} for 2 min over the reference and RNA surface.

At the end of each injection, the dissociation phase was set to 2 min, apart from the last one, which lasted for 20 min.

For data processing, data were double referenced by subtracting both the data obtained from the reference surface and the buffer response on the RNA surface to remove systematic noise and instrument drift. The data were fit with the software BIAevaluation 4.1, assuming a simple 1:1 association model.

Hydroxyl Radical Footprint Experiment. In order to obtain an independent estimate of the kinetic rate k_F of RNA folding (eq 2b), we used $OH^•$ footprint experiments.[23] The aptamer domain of the TPP riboswitch of the *E. coli thiC* gene was cloned under the control of the T7 RNA polymerase promoter. Linearized plasmids were used for *in vitro* transcription by T7 RNA polymerase according to usual protocols. The RNA products were further purified on a PAC100 column (Dionex, Thermo Fischer Science), and relevant fractions were washed and concentrated on a Centricon 10K (Millipore). After ^{32}P 5′-radiolabeling, the RNA was submitted to the renaturation procedure described for SPR experiments. The RNA was mixed with TPP (4 μM) during variable times and then probed by $OH^•$ radicals for 15 ms on a quench flow apparatus (Kintek RQF-3).

The cleavage products were resolved on 10% polyacrylamide gels in denaturing conditions. Gels were dried, exposed on imaging plates, and scanned on a Bioimage Analyser (Fuji Photo Film Co., Ltd.). In order to quantify the intensity of cleavage from the gels, we have developed our own software. Essentially, the method in use is analogous to previously described methods,[31−33] but with specificities that make it of interest. The result for the kinetics of cleavage of a representative set of residues is shown in Figure S9. Usually, the processing of such kinetic data is performed by considering each curve separately. However, we did not follow this method, and, in line with the method used for kinITC (eqs 2, 9, and 11), we have developed a new global method that allows fitting all available kinetic curves at once with very few free parameters (to be published).

■ ASSOCIATED CONTENT

Supporting Information

Web site, instrument response time, mixing time, equilibration time, range of application of kinITC, Van't Hoff equation, baseline correction, additional figures, quantitative results. This material is available free of charge via the Internet at http://pubs.acs.org.

■ AUTHOR INFORMATION

Corresponding Author

p.dumas@ibmc-cnrs.unistra.fr

Present Addresses

[‡]Institute of Organic Chemistry, Leopold Franzens University, Innsbrück, Austria

[†]Université de Strasbourg, UMR7242 du CNRS, F67412 Illkirch, France.

Author Contributions

[§]These authors contributed equally.

■ ACKNOWLEDGMENTS

We acknowledge P. Wolff for technical assistance. Nevirapine reagent was obtained through the NIH AIDS Research and Reference Reagent Program, Division AIDS, NIAID, NIH. This work was supported by the Agence Nationale de la Recherche (ANR-08-PCVI-0016-10).

■ REFERENCES

(1) Falconer, R. J.; Penkova, A.; Jelesarov, I.; Collins, B. M. *J. Mol. Recognit.* **2008**, *23*, 395.

(2) Freire, E.; Mayorga, O. L.; Straume, M. *Anal. Chem.* **1990**, *62*, 950.

(3) Chaires, J. B. *Annu. Rev. Biophys.* **2008**, *37*, 135.

(4) Bianconi, M. L. *Biophys. Chem.* **2007**, *126*, 59.

(5) Berger, R. L.; Mudd, C. P.; Clem, T.; Kolobow, T.; Beile, E.; Simons, P. C.; Michel, S.; McClintock, W. *J. Biochem. Biophys. Methods* **1989**, *18*, 113.

(6) Morin, P. E.; Freire, E. *Biochemistry* **1991**, *30*, 8494.

(7) Bianconi, M. L. *J. Biol. Chem.* **2003**, *278*, 18709.

(8) Merluzzi, V. J.; Hargrave, K. D.; Labadia, M.; Grozinger, K.; Skoog, M.; Wu, J. C.; Shih, C. K.; Eckner, K.; Hattox, S.; Adams, J. *Science* **1990**, *250*, 1411.

(9) Rodionov, D. A.; Vitreschak, A. G.; Mironov, A. A.; Gelfand, M. S. *J. Biol. Chem.* **2002**, *277*, 48949.

(10) Winkler, W.; Nahvi, A.; Breaker, R. R. *Nature* **2002**, *419*, 952.

(11) Serganov, A.; Polonskaia, A.; Phan, A. T.; Breaker, R. R.; Patel, D. J. *Nature* **2006**, *441*, 1167.

(12) Wickiser, J. K.; Winkler, W. C.; Breaker, R. R.; Crothers, D. M. *Mol. Cell* **2005**, *18*, 49.

(13) Wickiser, J. K.; Cheah, M. T.; Breaker, R. R.; Crothers, D. M. *Biochemistry* **2005**, *44*, 13404.

(14) Geitmann, M.; Unge, T.; Danielson, U. H. *J. Med. Chem.* **2006**, *49*, 2375.

(15) Ren, J.; Esnouf, R.; Garman, E.; Somers, D.; Ross, C.; Kirby, I.; Keeling, J.; Darby, G.; Jones, Y.; Stuart, D.; et al. *Nat. Struct. Biol.* **1995**, *2*, 293.

(16) Kulshina, N.; Edwards, T. E.; Ferre-D'Amare, A. R. *RNA* **2010**, *16*, 186.

(17) Cooper, A. *Biophys. Chem.* **2005**, *115*, 89.

(18) Mikulecky, P. J.; Feig, A. L. *Biopolymers* **2006**, *82*, 38.

(19) Thore, S.; Leibundgut, M.; Ban, N. *Science* **2006**, *312*, 1208.

(20) Kawasaki, T.; Miyata, I.; Esaki, K.; Nose, Y. *Arch. Biochem. Biophys.* **1969**, *131*, 223.

(21) Leonardi, R.; Roach, P. L. *J. Biol. Chem.* **2004**, *279*, 17054.

(22) Nosaka, K.; Onozuka, M.; Konno, H.; Kawasaki, Y.; Nishimura, H.; Sano, M.; Akaji, K. *Mol. Microbiol.* **2005**, *58*, 467.

(23) Shcherbakova, I.; Mitra, S.; Beer, R. H.; Brenowitz, M. *Nucleic Acids Res.* **2006**, *34*, e48.

(24) Balasubramanian, B.; Pogozelski, W. K.; Tullius, T. D. *Proc. Natl. Acad. Sci. U.S.A.* **1998**, *95*, 9738.

(25) Schubert, F.; Zettl, H.; Hafner, W.; Krauss, G.; Krausch, G. *Biochemistry* **2003**, *42*, 10288.

(26) Wolf, L. K.; Gao, Y.; Georgiadis, R. M. *J. Am. Chem. Soc.* **2007**, *129*, 10503.

(27) Jecklin, M. C.; Schauer, S.; Dumelin, C. E.; Zenobi, R. *J. Mol. Recognit.* **2009**, *22*, 319.

(28) It may be noted, however, that these two criteria are not fully independent since a low global K_d value more or less implies a low k_{off}(global) value.

(29) Freisz, S.; Bec, G.; Radi, M.; Wolff, P.; Crespan, E.; Angeli, L.; Dumas, P.; Maga, G.; Botta, M.; Ennifar, E. *Angew. Chem., Int. Ed.* **2010**, *49*, 1805.

(30) Radi, M.; Maga, G.; Alongi, M.; Angeli, L.; Samuele, A.; Zanoli, S.; Bellucci, L.; Tafi, A.; Casaluce, G.; Giorgi, G.; Armand-Ugon, M.; Gonzalez, E.; Este, J. A.; Baltzinger, M.; Bec, G.; Dumas, P.; Ennifar, E.; Botta, M. *J. Med. Chem.* **2009**, *52*, 840.

(31) Das, R.; Laederach, A.; Pearlman, S. M.; Herschlag, D.; Altman, R. B. *RNA* **2005**, *11*, 344.

(32) Takamoto, K.; Chance, M. R.; Brenowitz, M. *Nucleic Acids Res.* **2004**, *32*, E119.

(33) Laederach, A.; Das, R.; Vicens, Q.; Pearlman, S. M.; Brenowitz, M.; Herschlag, D.; Altman, R. B. *Nat. Protoc.* **2008**, *3*, 1395.